

# Direct Detection of the Radical Cation of 2,6-Di-*tert*-butyl-4-methylphenol Generated by Electron-Transfer Oxidation with Matrix Alkyl Halide Cation Radicals. A Low-Temperature EPR and UV–VIS Optical Absorption Study†

Valentin E. Zubarev and Ortwin Brede\*

Max Planck Society, Group Time Resolved Spectroscopy at the University of Leipzig, Permoserstr. 15, 04303 Leipzig, Germany

Zubarev, V. E. and Brede, O., 1997. Direct Detection of the Radical Cation of 2,6-Di-*tert*-butyl-4-methylphenol Generated by Electron-Transfer Oxidation with Matrix Alkyl Halide Cation Radicals. A Low-Temperature EPR and UV–VIS Optical Absorption Study. – Acta Chem Scand. 51: 224–228. © Acta Chemica Scandinavica 1997.

Electron-transfer oxidation of 2,6-di-*tert*-butyl-4-methylphenol (ArOH, **1**) by matrix (RHal) radical cations (RHal=Freon-113, Bu<sup>•</sup>Cl and Bu<sup>•</sup>Cl) results in the formation of the radical cation ArOH<sup>•+</sup> (**2**) as a primary intermediate directly observed during EPR and UV–VIS optical absorption measurements at 77 K. In the glassy matrix of Bu<sup>•</sup>Cl the radical cation ArOH<sup>•+</sup> exhibits a broad absorption band with  $\lambda_{\text{max}}=450$  nm ( $\epsilon/\text{dm}^3 \text{ mol}^{-1} \text{ cm}^{-1} 2.1 \times 10^3$ ). The EPR spectrum of ArOH<sup>•+</sup> at 77 K is characterised by isotropic splitting from the freely rotating CH<sub>3</sub> group and anisotropic splitting from the hydrogen atom in the OH group. Upon warming in the temperature range 77–103 K, deprotonation of ArOH<sup>•+</sup> and dedeuteriation of its deuterium-substituted analog ArOD<sup>•+</sup> resulting in the formation of the 2,6-di-*tert*-butyl-4-methylphenoxy radical ArO<sup>•</sup> (**4**), was directly observed by EPR and optical absorption measurements in all matrices studied.

The antioxidative properties of (sterically hindered) phenols can be understood when it is considered that phenols can act as electron and as hydrogen atom donors. Abstraction of a hydrogen atom from the OH group results directly in a phenoxy radical.<sup>1</sup> Under electron transfer oxidative conditions, in most cases phenoxy radicals were also detected as the first observable transients,<sup>2</sup> which can only be explained by suggesting a radical cation as a very unstable intermediate.

Because of the very low pK value<sup>2a,3</sup> of phenol radical cations they could be observed in aqueous or polar solutions only under strongly acidic conditions. Thus, cation radicals of various substituted phenols were characterised by their steady-state solution EPR spectra in sulfuric acid solutions<sup>3</sup> or in the presence<sup>4a-c</sup> of strong Lewis acids (AlCl<sub>3</sub> in CH<sub>3</sub>NO<sub>2</sub> or CH<sub>2</sub>Cl<sub>2</sub>). In both cases<sup>3,4a-c</sup> radical cations are in a reversible protonation equilibrium with the phenoxy radicals and their formation in the primary electron transfer oxidative step could

not be proved. Cyclic voltammetry on some phenols<sup>4d</sup> in acidic media (CH<sub>2</sub>Cl<sub>2</sub> with 10% FSO<sub>3</sub>H) has also provided evidence for the formation of radical cations.

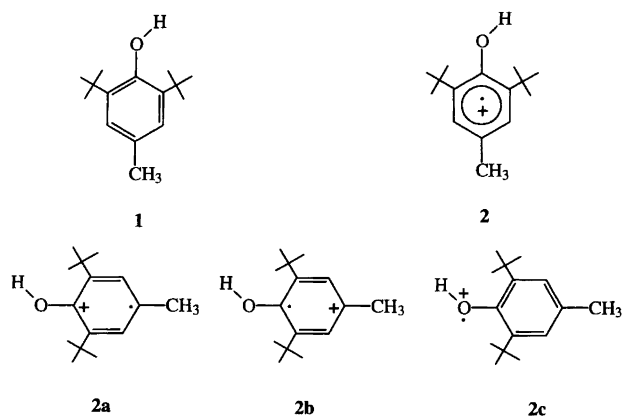
In the case of phenols that contain *para*-substituents with a high affinity for protons, such as amino groups, photoionisation combined with optical matrix isolation spectroscopy has indicated the existence<sup>2b,5a</sup> of radical cations. Furthermore, *p*-aminophenol radical cations could also be identified in strongly acidic solution using<sup>5b</sup> time-resolved Raman resonance spectroscopy. The photolytic and radiolytic ionisation of phenol itself in argon matrices yielded optical absorption spectra which have been interpreted<sup>6</sup> to be due to PhOH<sup>•+</sup> and PhO<sup>•</sup>.

To avoid structural peculiarities leading to isomerisation involving the *ortho*-position and charge localisation in the *para*-position, we studied the ionisation of sterically hindered phenols by means of pulse radiolysis. Electron transfer oxidation of some of these phenols in non-polar solutions at room temperature indicates that phenoxy radicals are really subsequent products of very short-lived cation radicals.<sup>7</sup> In order to gain deeper insight into the chemistry and structure of the primary oxidised

† Lecture held at the 14th International Conference on Radical Ions, Uppsala, Sweden, July 1–5, 1996.

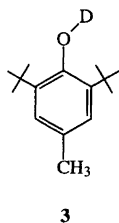
\* To whom correspondence should be addressed.

intermediates we have performed a low temperature matrix isolation investigation of the radical cations derived from the sterically hindered 2,6-di-*tert*-butyl-4-methylphenol (ArOH, **1**). The radical cations were generated by  $\gamma$ -radiolysis of ArOH dissolved in glass-forming matrices of  $\text{CF}_2\text{ClCFCl}_2$  (Freon-113),  $\text{Bu}^s\text{Cl}$  and  $\text{Bu}^t\text{Cl}$ . Using two different detection techniques – EPR and UV–VIS optical absorption spectroscopy – we report here upon the characterisation of the radical cations  $\text{ArOH}^{\cdot+}$  (**2**).



## Experimental

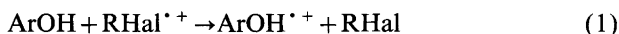
First-derivative X band EPR measurements and  $\gamma$ -irradiation (dose 5 kGy) of the frozen, degassed solutions were performed as described in our previous work.<sup>8</sup> A copper cryostat was used for the annealing of the irradiated samples at various temperatures. After annealing (cf. Ref. 9) the samples for 10 min they were recooled to 77 K for EPR or UV–VIS optical absorption measurements. Absorption spectra in frozen glassy matrices of  $\text{Bu}^s\text{Cl}$  at 77 K were measured for samples in Suprasil quartz cells ( $1 \times 10 \times 30 \text{ mm}^3$ ) using a Shimadzu UV–VIS Scanning Spectrophotometer UV-2101PC according to procedure outlined in Ref. 10(a). The experimental error in the absorbance measurements was estimated to be 10–15%.



**Chemicals.** 2,6-Di-*tert*-butyl-4-methylphenol (ArOH, **1**) from Bayer (Leverkusen) was used as received. 2,6-Di-*tert*-butyl-4-methyl-1-deuteriophenol (ArOD, **3**) was obtained from ArOH by means of a deuterium exchange reaction with excess  $\text{C}_2\text{H}_5\text{OD}$ . NMR spectral data confirmed more than 90% deuterium in ArOD. Freon-113 (*puriss.* Genetron<sup>®</sup> 113, Fluka),  $\text{Bu}^s\text{Cl}$  and  $\text{Bu}^t\text{Cl}$  (both from Aldrich) were used as described in Ref. 8.

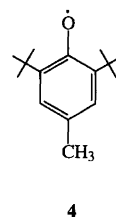
## Results and discussion

**Low temperature EPR studies.** Since the ionisation potential ( $E_i$ ) of ArOH (ArOD) is lower<sup>‡</sup> than that of the matrices studied,<sup>10</sup>  $\gamma$ -irradiation of ArOH in frozen halogenated matrices (RHal) is expected to lead to the formation of the radical cations  $\text{ArOH}^{\cdot+}$ <sup>10,11</sup> as a result of an electron transfer from the solute molecules to the matrix radical cations  $\text{RHal}^{\cdot+}$  according to eqn. (1).



Secondary electrons generated in matrices during  $\gamma$ -irradiation at 77 K are completely scavenged by matrix molecules resulting in the formation of matrix-derived radicals as well as  $\text{Cl}^-$  anions.<sup>10,11</sup> In the case of Freon-113, matrix-derived  $\text{CF}_2\text{ClCFCl}^{\cdot}$  radicals could not strongly contribute to the observed EPR signal because of the anisotropic line broadening.<sup>11</sup>

Table 1 shows the hyperfine coupling constants for all investigated species. The EPR spectrum of irradiated ArOH ( $0.05 \text{ mol dm}^{-3}$ ) in a Freon-113 matrix [Fig. 1(a)] we assign to the radical cation  $\text{ArOH}^{\cdot+}$ . This asymmetric, near to 1:3:3:1 quartet signal exhibits splitting from three equivalent protons in the  $\text{CH}_3$  group. The asymmetry of the EPR spectrum and the additional doublet features are due to the anisotropic dipole–dipole interaction of the unpaired electron on the 2p oxygen orbital with the H atom in the OH group (cf. Refs. 12).



In fact, the EPR spectrum of the deuterium-substituted radical cation  $\text{ArOD}^{\cdot+}$  in Fig. 1(b) shows a well-resolved 1:3:3:1 isotropic splitting from the methyl protons only,<sup>§</sup> thus indicating a freely rotating  $\text{CH}_3$  group, as in the phenoxy radical<sup>13</sup>  $\text{ArO}^{\cdot}$  (**4**). A well-resolved symmetrical spectrum of  $\text{ArOD}^{\cdot+}$  indicates furthermore that anisotropy of the  $g$ -tensor as well as hyperfine interaction with the two *meta*-protons (Table 1) of the aromatic ring in  $\text{ArOD}^{\cdot+}$  and, hence, in  $\text{ArOH}^{\cdot+}$ , are small and contribute to the linewidth of the EPR spectrum. The hyperfine coupling constants from the  $\text{CH}_3$  group in  $\text{ArOD}^{\cdot+}$  (and  $\text{ArOH}^{\cdot+}$ ) are in agreement with those measured<sup>4b,c</sup> in solution EPR spectra for these cation radicals (see Table 1).

$\text{ArOH}^{\cdot+}$  is a typical<sup>15</sup>  $\pi$ -electron radical cation with charge and spin delocalised over the aromatic ring and

<sup>‡</sup>  $E_i$  for ArOH and ArOD are not known. In this work we assume that they have the same  $E_i$  (8.52 eV) as PhOH (see Ref. 6).

<sup>§</sup> The hyperfine coupling constant for deuterium should be 6.514 times smaller<sup>14</sup> and hence it contributes to the linewidth of the EPR spectrum.

Table 1. EPR parameters for ArOH<sup>•+</sup>, ArOD<sup>•+</sup> and ArO<sup>•</sup> in Freon-113.

Radical	g-Factor	Hyperfine coupling/G			T/K	Ref.
		a <sub>H</sub> (CH <sub>3</sub> )	a <sub>H</sub> (meta-H)	a <sub>H</sub> (OH)		
ArOH <sup>•+</sup>	g <sub>  </sub> = 2.0035	14.3		A <sub>  </sub> = 10.0	77	
ArOD <sup>•+</sup>		14.3			77	
ArOH <sup>•+</sup>		14.19	0.89 (1 H)	3.72	213	4(c)
		14.43	0.8 (1 H)	3.6	213	4(b)
ArO <sup>•</sup>	g <sub>iso</sub> = 2.0054	11.1			77	
		11.2	1.70		298	
		11.0	1.65		298	1

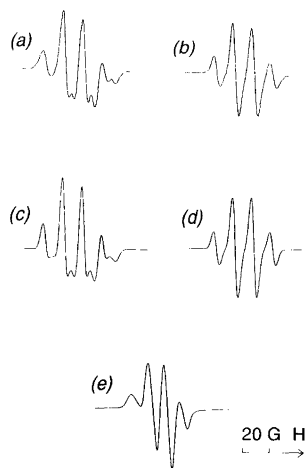


Fig. 1. EPR spectra of radical cations ArOH<sup>•+</sup> (a) and ArOD<sup>•+</sup> (b) in Freon-113 matrix compared with computer-simulated spectra (c) and (d), respectively. Deprotonation of both radical cations results in the phenoxyl radical ArO<sup>•</sup> (e). All spectra were recorded at 77 K.

2p orbitals of the oxygen atom as described by the mesomeric structures **2a**, **2b** and **2c**. An increase (about 29%) of the methyl coupling constant  $a_{\text{H}}(\text{CH}_3)$  in ArOH<sup>•+</sup> and ArOD<sup>•+</sup>, in comparison with that for the corresponding phenoxyl radical ArO<sup>•</sup> (Table 1), indicates increased spin density at the C-4 position of the aromatic ring in the radical cation. This is in line with the results for other substituted phenol radical cations.<sup>3,4</sup> The g-factor for the radical cation ArOD<sup>•+</sup> is smaller than that for the phenoxyl radical ArO<sup>•</sup> (which is observed at lower magnetic field, see below), thus further supporting the identification of the radical cation ArOH<sup>•+</sup> (cf. Ref. 3).

With  $A_{\parallel}(\text{H})$  and  $g_{\parallel}$  determined directly from the experimental EPR spectrum of ArOH<sup>•+</sup>, and assuming an axially symmetric anisotropic hyperfine tensor for the hydrogen atom of the OH group [cf. Ref. 12(b)], the EPR spectra of the ArOH<sup>•+</sup> and ArOD<sup>•+</sup> radical cations were computer-simulated in agreement with experiment [Figs. 1(c) and (d), respectively] using  $A_{\perp} = 2 \text{ G}$ ,  $g_{\perp} = 2.0050$  and a linewidth of 3.2 G.

EPR measurements performed with ArOH in a Bu<sup>•</sup>Cl matrix also clearly demonstrate the formation of ArOH<sup>•+</sup>. Although in this case both ArOH<sup>•+</sup> and

matrix-derived butyl radicals contribute to the EPR spectrum, the characteristic 1:3:3:1 quartet of ArOH<sup>•+</sup> is clearly observed (see insert in Fig. 2). Similar results were obtained in a Bu<sup>•</sup>Cl matrix (spectra not shown).

Upon annealing of irradiated matrices at 88 K, the intensity of the EPR signal from the radical cations diminished and the slightly asymmetric 1:3:3:1 quartet signal (shifted to low field) of the phenoxyl radicals<sup>13</sup> ArO<sup>•</sup> (**4**) grew, in all matrices studied. Two different paramagnetic species – ArOH<sup>•+</sup> (ArOD<sup>•+</sup>) and ArO<sup>•</sup> – were simultaneously observed in the EPR spectra upon annealing in the temperature range up to 107 K. After 10 min annealing at 107 K only the phenoxyl radical ArO<sup>•</sup> was observed in the EPR spectrum in both ArOH and ArOD samples, as shown in Fig. 1(e) for the Freon-113 matrix. This indicates the deprotonation of the radical cations ArOH<sup>•+</sup> and ArOD<sup>•+</sup> according to eqns. (2a) and (2b). The deprotonation is nearly quantit-

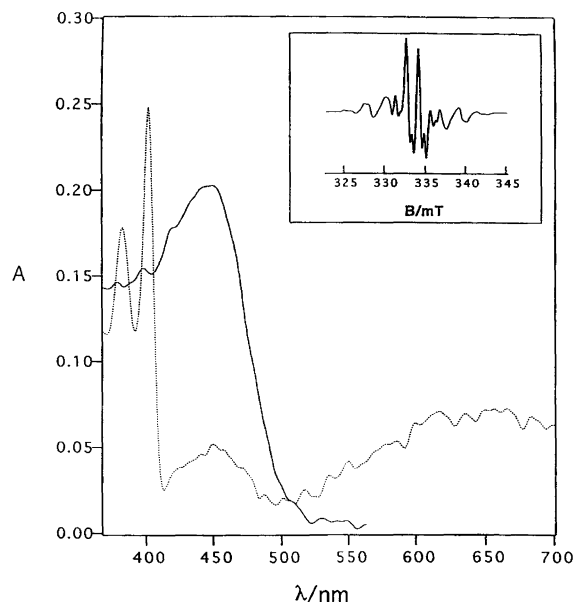


Fig. 2. UV-VIS optical absorption spectra of the radical cation ArOH<sup>•+</sup> (bold curve) and phenoxyl radical ArO<sup>•</sup> (dotted curve) in an irradiated Bu<sup>•</sup>Cl glassy matrix. Insert: EPR spectrum taken immediately after irradiation at 77 K; the central part (bold curve) of the EPR spectrum clearly shows the characteristic quartet due to the radical cations ArOH<sup>•+</sup>.

ative, based on the EPR measurements in the Freon-113 matrix.



Upon further warming, the phenoxyl radicals  $\text{ArO}^{\cdot}$  decayed (more than 90%) in all matrices studied, owing to their reactions with matrix-derived radicals and to reversible dimerisation<sup>2a,16</sup> into molecular metastable dimeric products. After melting the irradiated matrices, a weak EPR signal due to the phenoxyl radicals  $\text{ArO}^{\cdot}$  (Table 1) could be observed at room temperature in the first few minutes.

*Low temperature UV-VIS optical absorption measurements.* In contrast with the pure matrices,<sup>10</sup> glassy matrices containing dissolved  $\text{ArOH}$  became intense yellow-green in color upon irradiation. For the optical absorption measurements  $\text{Bu}^{\text{c}}\text{Cl}$  was chosen as the matrix, due to the fact that upon being frozen it results in good glasses.<sup>10a</sup> Fig. 2 (bold curve) shows the absorption spectrum immediately after irradiation of  $\text{ArOH}$  (0.05 mol  $\text{dm}^{-3}$ ) in a glassy  $\text{Bu}^{\text{c}}\text{Cl}$  matrix. Based on the EPR results (above) we assign the broad absorption band with  $\lambda_{\text{max}}=450$  nm and a shoulder at  $\lambda=295$  nm (not shown) to the absorption spectrum of the radical cation  $\text{ArOH}^{\cdot+}$ . This double-band absorption spectrum is quite similar to that of the phenol radical cation  $\text{PhOH}^{\cdot+}$  in a frozen argon matrix<sup>6</sup> – a broad absorption band at  $\lambda=420$  nm and a shoulder at 275 nm. The red shift of the  $\text{ArOH}^{\cdot+}$  absorption could be due to matrix and alkyl-substitution effects.

The changes in optical absorption upon warming of irradiated solutions parallel those in the EPR spectra. Two characteristic peaks<sup>2</sup> of the phenoxyl radical  $\text{ArO}^{\cdot}$  at  $\lambda_{\text{max}}=401$  nm and 382 nm are clearly seen in the absorption spectrum taken after the decay of the radical cation  $\text{ArOH}^{\cdot+}$  upon warming up to 107 K (Fig. 2, dotted curve). This is in agreement with the EPR results described above.

Assuming that  $\text{ArO}^{\cdot}$  resulted only from the deprotonation [see eqns. (2a) and (2b)] of the radical cations  $\text{ArOH}^{\cdot+}$ , an estimate of the extinction coefficient ( $\epsilon$ ) for the radical cation  $\text{ArOH}^{\cdot+}$  could be made directly from the absorption spectra. Using<sup>¶</sup> for  $\text{ArO}^{\cdot}$  an  $\epsilon$ -value at  $\lambda_{\text{max}}=401$  nm of  $4.3 \times 10^3 \text{ dm}^3 \text{ mol}^{-1} \text{ cm}^{-1}$ , this gives, for the broad absorption band of the cation radical  $\text{ArOH}^{\cdot+}$  at  $\lambda_{\text{max}}=450$  nm,  $\epsilon=2.1 \times 10^3 \text{ dm}^3 \text{ mol}^{-1} \text{ cm}^{-1}$ .

¶ The  $\epsilon$ -value for  $\text{ArO}^{\cdot}$  at  $\lambda_{\text{max}}=401$  nm was calculated from the  $k/\epsilon$  ratio determined by Land and Porter [Ref. 2(b)] and the (extrapolated to room temp.) decay rate constant measured by Rütgege and Fischer (Ref. 16). This value is in good agreement with that ( $4.13 \times 10^3 \text{ dm}^3 \text{ mol}^{-1} \text{ cm}^{-1}$ ) measured<sup>17</sup> for the analogous 2,4,6-trimethylphenoxyl radical.

## Conclusions

Electron transfer oxidation of simple hindered phenols such as  $\text{ArOH}$  and  $\text{ArOD}$  by matrix radical cations results in the formation of the radical cations  $\text{ArOH}^{\cdot+}$  and  $\text{ArOD}^{\cdot+}$  as primary intermediates directly observed during low-temperature EPR and UV-VIS optical absorption measurements. Deprotonation of  $\text{ArOH}^{\cdot+}$  and  $\text{ArOD}^{\cdot+}$  according to eqns. (2a) and (2b) yields phenoxyl radicals  $\text{ArO}^{\cdot}$ . This reaction was observed by EPR and optical absorption spectroscopy in different halogenated matrices in the temperature range 77–103 K.

Thus, electron transfer oxidation of phenols followed by deprotonation of the resultant radical cation is a two-step reaction route that explains the appearance of phenoxyl radicals under conditions excluding hydrogen abstraction from the OH group of phenol molecules. Both steps are of importance for phenol chemistry in biological systems as well as for the chemistry of sterically hindered phenolic antioxidants and stabilisers.

## References

1. Becconsall, J. K., Clough, S. and Scott, G. *Proc. Chem. Soc.* (1959) 308; Bennett, J. E. *Nature* 186 (1960) 385.
2. (a) Land, E. J., Porter, G. and Strachan, E. *Trans. Faraday Soc.* 57 (1961) 1885; (b) Land, E. J. and Porter, G. *Trans. Faraday Soc.* 59 (1963) 2016; (c) Land, E. J. and Ebert, M. *Trans. Faraday Soc.* 63 (1967) 1181; (d) Bansal, K. M. and Fessenden, R. W. *Radiat. Res.* 67 (1976) 1.
3. Dixon, W. T. and Murphy, D. *J. Chem. Soc., Faraday Trans. 2* 72 (1976) 1221; Dixon, W. T., Kok, P. M. and Murphy, D. *J. Chem. Soc., Faraday Trans. 2* 73 (1977) 709.
4. (a) Sullivan, P. D. and Bolton, J. R. *J. Am. Chem. Soc.* 90 (1968) 5366; (b) Pochodenko, V. D., Khizhnyi, V. A., Koschekko, V. G. and Schkrebti, O. I. *Dokl. Akad. Nauk SSSR* 210 (1973) 640; (c) Nemoto, F., Tsuzuki, N., Mukai, K. and Ishizu, K. *J. Phys. Chem.* 85 (1981) 2450; (d) Hammerich O., Parker V. D. and Ronlán A. *Acta Chem. Scand., Ser. B* 30 (1976) 89.
5. (a) Kimura, K., Yoshinaga, K. and Tsubomura, H. *J. Phys. Chem.* 71 (1967) 4485; (b) Sun, Q., Tripathi, G. N. R. and Schuler, R. H. *J. Phys. Chem.* 94 (1990) 6273.
6. Kesper, K., Diehl, F., Simon, J. G. G., Specht, H. and Schweig, A. *Chem. Phys.* 153 (1991) 511.
7. Brede, O., Orthner, H. and Hermann, R. *Chem. Phys. Lett.* 229 (1994) 571; Brede, O., Orthner, H., Zubarev, V. and Hermann, R. *J. Phys. Chem.* 100 (1996) 7097.
8. Zubarev, V. E. and Brede, O. *J. Chem. Soc., Perkin Trans. 2* (1994) 1821.
9. Malone, M. E., Symons, M. C. R. and Parker, A. W. *J. Chem. Soc., Perkin Trans. 2* (1993) 2067.
10. (a) Hamill, W. H. In: Kaiser, E. T. and Kevan, L., Eds., *Radical Ions*, Wiley-Interscience, New York 1968, p. 321; (b) Hurni, B. and Bühler, R. E. *Radiat. Phys. Chem.* 15 (1980) 231.
11. Shida, T., Egawa, Y., Kubodera, H. and Kato, T. *J. Chem. Phys.* 73 (1980) 5963; Symons, M. C. R. and McLauchlan, K. A. *Faraday Discuss. Chem. Soc.* 78 (1984) 7; Lindgren, M. and Lund, A. *J. Chem. Soc., Faraday Trans. 1* 83 (1987) 1815; Lindgren, M., Matsumoto, M. and Shiotani, M. *J. Chem. Soc., Perkin Trans. 2* (1992) 1397.
12. (a) Derbyshire, W. *Mol. Phys.* 5 (1962) 225; (b) Brustolon, M., Carbonera, D., Cassol, M. T. and Giacomenti, G. *Gazz. Chim. Ital.* 117 (1987) 149.
13. Clough, S. and Poldy, F. *J. Chem. Phys.* 51 (1969) 2076;

- Atherton, N. M. and Oliver, C. E. *J. Chem. Soc., Faraday Trans. 1* 84 (1988) 3257.
14. Lawler, R. G. and Fraenkel, G. K. *J. Chem. Phys.* 49 (1968) 1126.
15. McConnell, H. M. and Chesnut, D. B. *J. Chem. Phys.* 28 (1958) 107.
16. Rügge, D. and Fischer, H. *J. Chem. Soc., Faraday Trans. 1* 84 (1988) 3187.
17. Grabner, G., Köhler, G., Marconi, G., Monti, S. and Venuti, E. *J. Phys. Chem.* 94 (1990) 3609.

Received July 1, 1996.